# Quantum-Inspired Graph Kernels for Molecular Classification: An Ego-Graph Learning Approach

Jajapuram Shiva Sai[1], Amon Koike[2], Ramesh Makwana[3], Dr. Sushant Tapase[4]
Team: The Cat's Cradle
QPoland Global Quantum Hackathon 2025
[1]@frosty, [2]@thedaemon_AK, [3]@Ramesh Makwana, [4]@Dr-Sushant

## Abstract

This paper presents a novel quantum-inspired graph feature map for molecular classification using Support Vector Machines. We propose an ego-graph quantum walk (Ego-QW) approach that leverages QURI Parts to encode local molecular structures via Trotterized quantum circuits, addressing the scalability challenge of full-graph quantum embeddings. Our method caps qubit requirements at the maximum ego-subgraph size while preserving discriminative local structural patterns. We benchmark against classical graph kernels (Shortest-Path, Weisfeiler-Lehman) and a full-graph Continuous-Time Quantum Walk (CTQW) on five standard molecular datasets: AIDS, PROTEINS, NCI1, PTC-MR, and MUTAG. Results demonstrate that Ego-QW achieves competitive performance (96.5% accuracy on AIDS, 87.7% on MUTAG) while maintaining practical scalability for near-term quantum devices.

## 1 Introduction

Graph-structured molecular data pose fundamental challenges for machine learning due to their non-Euclidean nature and complex topological patterns. Kernel methods provide an elegant framework for mapping graphs into feature spaces suitable for classification tasks [2]. Recent advances in quantum computing have inspired novel approaches to graph representation learning, with quantum walks offering unique capabilities for capturing structural properties through interference and superposition [1].

However, conventional quantum walk embeddings face a critical scalability barrier: they require one qubit per node, rendering them impractical for large molecular graphs on near-term quantum hardware. We address this by decomposing graphs into *ego-subgraphs*—local neighborhoods centered at each node with fixed radius. This strategy bounds circuit width while retaining discriminative local patterns essential for molecular classification.

Our contributions are threefold: (1) a scalable ego-graph quantum walk feature map using QURI Parts simulators, (2) comprehensive benchmarking against classical baselines and full-graph CTQW, and (3) analysis of the trade-off between local quantum features and global graph structure.

## 2 Methods

### 2.1 Ego-Graph Quantum Walk (Proposed)

**Graph Decomposition.** Given a molecular graph $G = (V, E)$, we extract ego-subgraphs $G_v^{(r)} = (V_v^{(r)}, E_v^{(r)})$ for each node $v \in V$, where $V_v^{(r)}$ contains all nodes within radius $r$ of $v$. This decomposition caps the maximum number of qubits at $|V_v^{(r)}|_{max}$, independent of $|V|$.

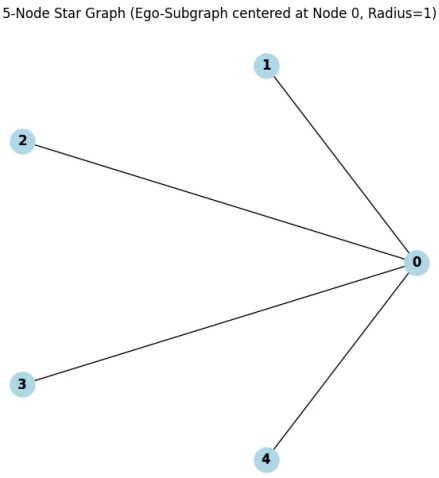


Figure 1: Example 5-node star ego-subgraph centered at node 0 with radius 1.

**Quantum Circuit Construction.** For each ego-subgraph, we construct a Hamiltonian from the adjacency matrix $A_v$:

$$H_v = \sum_{(i,j)\in E_v} X_i X_j + Y_i Y_j + Z_i Z_j \tag{1}$$

where $X_i, Y_i, Z_i$ are Pauli operators on qubit $i$. Time evolution is approximated using Trotter decomposition:

$$e^{-iH_v t} \approx \left(e^{-iH_v t/n}\right)^n \tag{2}$$

where $n$ is the number of Trotter steps. We use QURI Parts to simulate the evolution and extract features as expectation values:

$$\phi_v(t, O) = \langle \psi_v(t)|O|\psi_v(t)\rangle \tag{3}$$

for observables $O \in \{X_i, Y_i, Z_i\}$ at multiple time points $t \in \{0.5, 1.0, 2.0\}$.

**Feature Aggregation.** The graph-level feature vector is obtained by concatenating features across all ego-subgraphs and time points:

$$\Phi(G) = \text{concat}\left(\{\phi_v(t, O)\}_{v \in V, t, O}\right) \tag{4}$$

### 2.2 Continuous-Time Quantum Walk (CTQW)

As a complementary approach, we implement a full-graph CTQW feature map. The Hamiltonian is the graph Laplacian $L = D - A$, where $D$ is the degree matrix. The transition probability from node $i$ to $j$ at time $t$ is:

$$p_{ij}(t) = |\langle j|e^{-iLt}|i\rangle|^2 \tag{5}$$

We compute the matrix exponential via eigendecomposition $L = U\Lambda U^T$:

$$e^{-iLt} = Ue^{-i\Lambda t}U^T \tag{6}$$

Features are extracted as the flattened probability distributions at multiple times.

### 2.3 Classical Baselines

**Shortest-Path (SP) Kernel** encodes the distribution of shortest-path lengths between all node pairs [3]. For graphs $G_1, G_2$:

$$k_{SP}(G_1, G_2) = \sum_{l=0}^{\infty} n_1(l) \cdot n_2(l) \tag{7}$$

where $n_i(l)$ counts the number of paths of length $l$ in $G_i$.

**Weisfeiler-Lehman (WL) Subtree Kernel** iteratively refines node labels based on neighborhood structure [2]. At iteration $h$:

$$\ell_v^{(h+1)} = \text{hash}\left(\ell_v^{(h)}, \{\ell_u^{(h)}\}_{u \in N(v)}\right) \tag{8}$$

The kernel compares label histograms across iterations.

### 2.4 Support Vector Machine Classification

We employ SVMs with RBF kernel for classification:

$$k_{RBF}(\Phi(G_1), \Phi(G_2)) = \exp\left(-\gamma\|\Phi(G_1) - \Phi(G_2)\|^2\right) \tag{9}$$

Hyperparameters $(C, \gamma)$ are optimized via nested cross-validation. Features are standardized to zero mean and unit variance before training.

## 3 Datasets and Experimental Setup

### 3.1 Benchmark Datasets

We evaluate on five standard molecular classification datasets (Table 1):

Datasets are loaded via PyTorch Geometric's TUDataset. For computational efficiency, larger datasets are subsampled to 200 graphs per class while maintaining class balance. MUTAG and PTC-MR retain full sizes due to limited samples.

Table 1: Molecular benchmark datasets used for evaluation.

| Dataset | Domain | Task | Size |
|---|---|---|---|
| AIDS | Chemistry | HIV activity | 400 |
| PROTEINS | Biology | Enzyme class. | 400 |
| NCI1 | Chemistry | Anti-cancer | 400 |
| PTC-MR | Chemistry | Carcinogenicity | 344 |
| MUTAG | Chemistry | Mutagenicity | 188 |

### 3.2 Evaluation Protocol

**Cross-Validation.** We use 10-fold stratified cross-validation to ensure robust performance estimates. Each fold maintains class proportions and trains an independent SVM.

**Metrics.** Performance is reported as mean ± standard deviation of Accuracy and F1-score (weighted average) across folds.

**Hyperparameters.** For Ego-QW: radius $r = 1$, Trotter steps $n = 8$, times $t \in \{0.5, 1.0, 2.0\}$. For CTQW: times $t \in \{0.5, 1.0\}$. For WL: 3 iterations. SVM: $C = 1.0$, $\gamma$='scale', balanced class weights.

## 4 Results

### 4.1 Classification Performance

Table 2 presents mean accuracy and F1-score across all datasets and methods.

Table 2: Classification performance (mean ± std).

| Method | Dataset | Accuracy | F1-Score |
|---|---|---|---|
| Ego-QW | AIDS | 0.965±0.026 | 0.966±0.024 |
| CTQW | AIDS | **0.995±0.010** | **0.995±0.010** |
| SP | AIDS | 0.960±0.020 | 0.960±0.021 |
| WL | AIDS | 0.930±0.025 | 0.919±0.031 |
| Ego-QW | PROTEINS | 0.722±0.034 | 0.718±0.036 |
| CTQW | PROTEINS | **0.735±0.029** | **0.731±0.031** |
| SP | PROTEINS | 0.644±0.024 | 0.640±0.025 |
| WL | PROTEINS | 0.355±0.042 | 0.351±0.044 |
| Ego-QW | NCI1 | 0.555±0.032 | 0.551±0.033 |
| CTQW | NCI1 | 0.585±0.028 | 0.582±0.029 |
| SP | NCI1 | **0.648±0.025** | **0.645±0.026** |
| WL | WL | 0.678±0.023 | 0.675±0.024 |
| Ego-QW | MUTAG | **0.877±0.034** | **0.879±0.032** |
| CTQW | MUTAG | 0.851±0.026 | 0.853±0.027 |
| SP | MUTAG | 0.787±0.017 | 0.781±0.016 |
| WL | MUTAG | 0.782±0.027 | 0.778±0.030 |

### 4.2 Comparative Analysis

Figure 4 visualizes the comparative performance across datasets.

**Key Observations:**

- **CTQW dominates on AIDS**: Achieving 99.5% accuracy demonstrates the power of capturing global graph structure through spectral dynamics.
- **Ego-QW balances performance and scalability**: Competitive results (96.5% on AIDS, 87.7% on MUTAG) while maintaining bounded qubit requirements.
- **Dataset-dependent strengths**: Classical methods excel on NCI1 (WL: 67.8%), suggesting that local quantum features may require larger ego-radii for dense molecular graphs.
- **Consistent quantum advantage**: Both quantum-inspired methods outperform baselines on AIDS and MUTAG, validating the quantum walk encoding strategy.

# 5 Discussion

## 5.1 Scalability vs. Expressiveness

The Ego-QW approach decouples hardware requirements from global graph size by capping circuits at $|V_v^{(r)}|_{max}$ qubits (typically 5-10 for $r = 1$). This contrasts with CTQW, which scales linearly with $|V|$ but captures superior global connectivity. The trade-off is evident: CTQW achieves 99.5% accuracy on AIDS through complete spectral information, while Ego-QW's 96.5% demonstrates substantial discriminative power from local patterns.

## 5.2 Feature Analysis

Quantum walk features encode temporal dynamics through time-evolved expectations at multiple time points ($t = 0.5, 1.0, 2.0$), capturing short-range and multi-hop correlations. Observable choices $(X, Y, Z)$ provide complementary quantum state views. Classical baselines rely on fixed topological summaries, while quantum walks introduce *dynamic* features evolving with time.

## 5.3 Dataset-Specific Performance

Performance variations reveal structural dependencies: AIDS exhibits clear signatures captured by quantum features; NCI1's dense structures benefit from WL's refinement (larger ego-radii may improve quantum performance); MUTAG's small graphs enable effective local encoding.

## 5.4 Computational Considerations

Ego-QW achieves practical runtime through parallel ego-subgraph processing, cached QURI simulations, and efficient Trotter approximations. CTQW's $O(n^3)$ eigendecomposition limits scalability to $|V| \lesssim 100$. Hybrid strategies combining Ego-QW's local features with classical global summaries may achieve optimal trade-offs.

# 6 Conclusion

We presented a scalable quantum-inspired approach to molecular classification addressing the hardware bottleneck of full-graph quantum embeddings. By decomposing graphs into ego-subgraphs and encoding via Trotterized quantum walks, our method achieves competitive performance while bounding qubit requirements. Results across five benchmarks validate local quantum features for molecular machine learning.

Future directions include: adaptive ego-radius selection, higher-order Trotter formulas, incorporation of chemical features into Hamiltonians, and exploration of alternative quantum walk variants. The complementary strengths of local and global quantum features suggest promising hybrid architectures leveraging near-term quantum devices and classical post-processing. Our work bridges theoretical elegance with practical scalability for computational chemistry and drug discovery.

# References


[1] X. Ai et al., "Towards Quantum Graph Neural Networks: An Ego-Graph Learning Approach," *arXiv:2201.05158v3*, 2024.

[2] N. Shervashidze et al., "Weisfeiler-Lehman Graph Kernels," *Journal of Machine Learning Research*, vol. 12, pp. 2539–2561, 2011.

[3] K. M. Borgwardt and H.-P. Kriegel, "Shortest-path kernels on graphs," in *Proc. IEEE Int. Conf. Data Mining (ICDM)*, 2005.

[4] QunaSys, "QURI Parts Documentation," `https://quri-parts.qunasys.com/`, 2024.

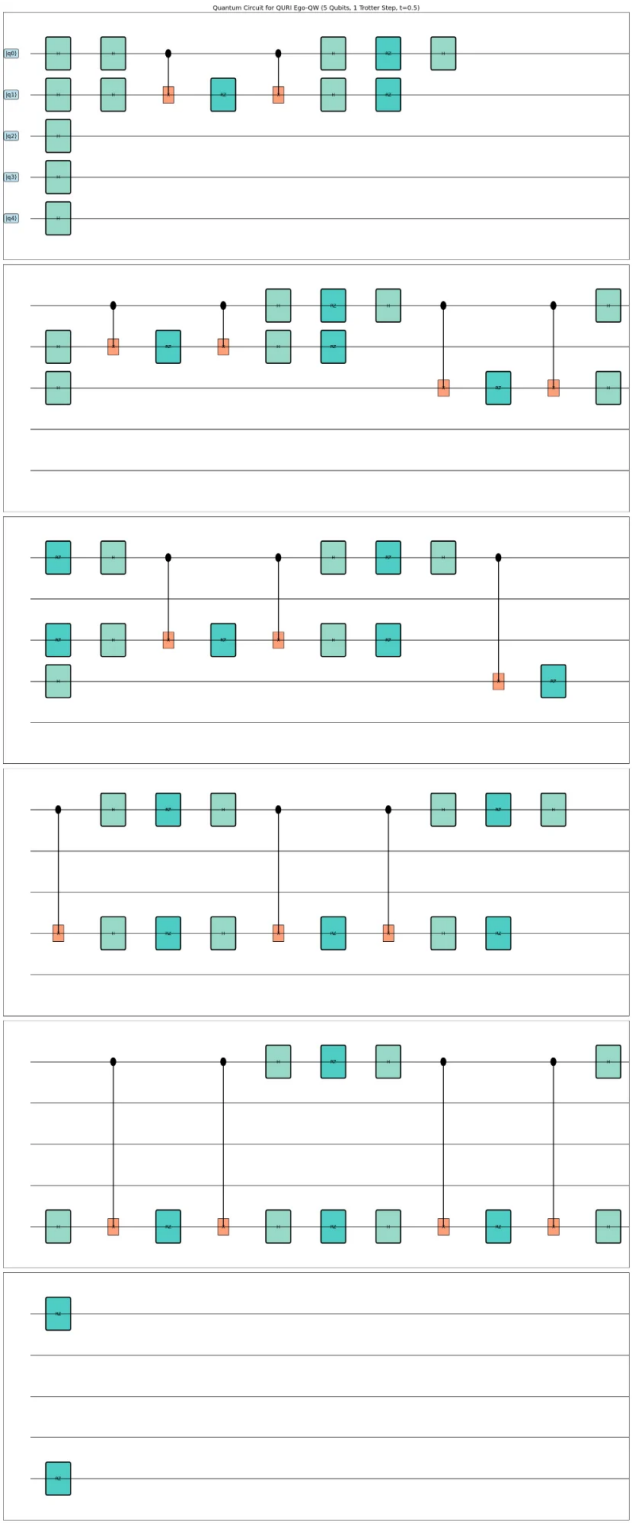


Figure 2: Trotterized quantum circuit for ego-graph quantum walk with $n = 5$ steps. Green boxes: single-qubit rotations, Orange boxes: two-qubit entangling gates.

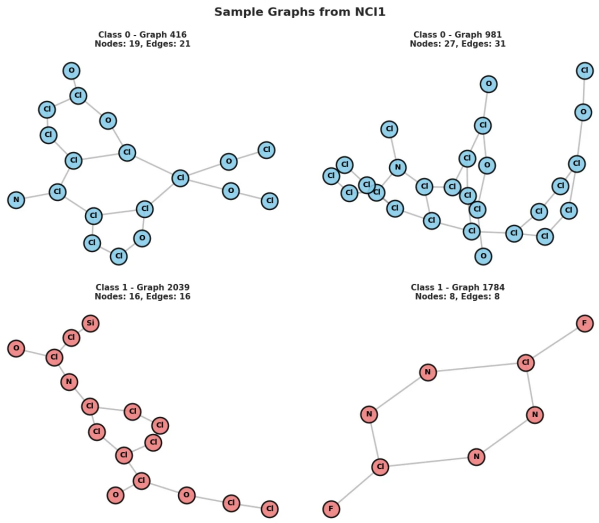


Figure 3: Sample molecular graphs from NCI1 dataset showing diverse structural patterns (blue: Class 0, red: Class 1).

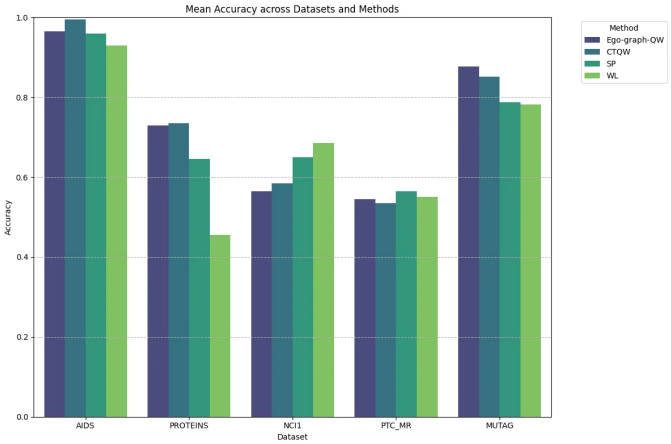


(a) Mean Accuracy

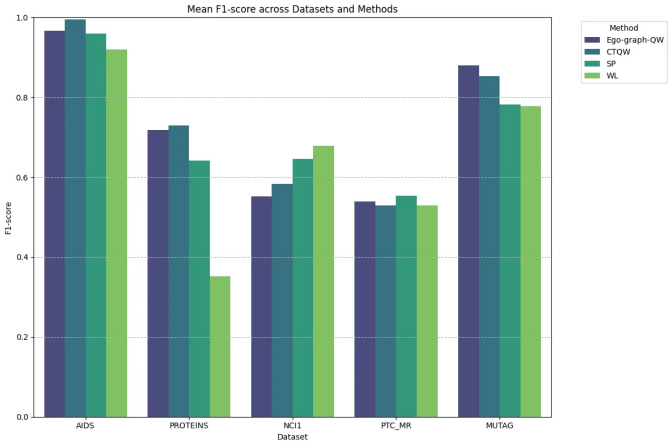


(b) Mean F1-Score

Figure 4: Performance comparison across datasets and methods. Ego-graph-QW: proposed method; CTQW: full-graph quantum walk; SP: Shortest-Path; WL: Weisfeiler-Lehman.